2012

Surface and Particle-Size Effects on Hydrogen Desorption from Catalyst-Doped MgH2

J. M. Reich
University of Illinois at Urbana-Champaign

Lin-Lin Wang
Ames Laboratory, llw@ameslab.gov

Duane D. Johnson
Iowa State University, ddj@iastate.edu

Surface and Particle-Size Effects on Hydrogen Desorption from Catalyst-Doped MgH2

Abstract
With their high capacity, light-metal hydrides like MgH2 remain under scrutiny as reversible H-storage materials, especially to develop control of H-desorption properties by decreasing size (ball-milling) and/or adding catalysts. By employing density functional theory and simulated annealing, we study initial H2 desorption from semi-infinite stepped rutile (110) surface and Mg31H62 nanoclusters, with(out) transition-metal catalyst dopants (Ti or Fe). While Mg31H62structures are disordered (amorphous), the semi-infinite surfaces and nanoclusters have similar single, double, and triple H-to-metal bond configurations that yield similar H-desorption energies. Hence, there is *no* size effect on desorption energetics with reduction in sample size, but dopants do reduce the H-desorption energy. All desorption energies are endothermic, in contrast to a recent report.

Keywords
Materials Science and Engineering

Disciplines
Condensed Matter Physics | Materials Science and Engineering | Physical Chemistry

Comments
Reprinted with permission from *J. Phys. Chem. C*, **2012**, *116* (38), pp. 20315–20320, doi:10.1021/jp304059c.

THE JOURNAL OF PHYSICAL CHEMISTRY C

Article

pubs.acs.org/JPCC

Surface and Particle-Size Effects on Hydrogen Desorption from Catalyst-Doped MgH_2

J. M. Reich,[†] Lin-Lin Wang,[‡] and Duane D. Johnson*[,‡,§,∥]

[†]Department of Chemistry, University of Illinois, 505 S. Matthews, Urbana, Illinois 61801, United States

[‡]Ames Laboratory, U.S. Department of Energy, Ames, Iowa 50011-3020, United States

[§]Department of Materials Science & Engineering, Iowa State University, Ames, Iowa 50011-2300, United States

[∥]Department of Materials Science & Engineering, University of Illinois, 1304 W. Green St., Urbana, Illinois 61801, United States

Supporting Information

ABSTRACT: With their high capacity, light-metal hydrides like MgH_2 remain under scrutiny as reversible H-storage materials, especially to develop control of H-desorption properties by decreasing size (ball-milling) and/or adding catalysts. By employing density functional theory and simulated annealing, we study initial H_2 desorption from semi-infinite stepped rutile (110) surface and $Mg_{31}H_{62}$ nanoclusters, with(out) transition-metal catalyst dopants (Ti or Fe). While $Mg_{31}H_{62}$ structures are disordered (amorphous), the semi-infinite surfaces and nanoclusters have similar single, double, and triple H-to-metal bond configurations that yield similar H-desorption energies. Hence, there is *no* size effect on desorption energetics with reduction in sample size, but dopants do reduce the H-desorption energy. All desorption energies are endothermic, in contrast to a recent report.

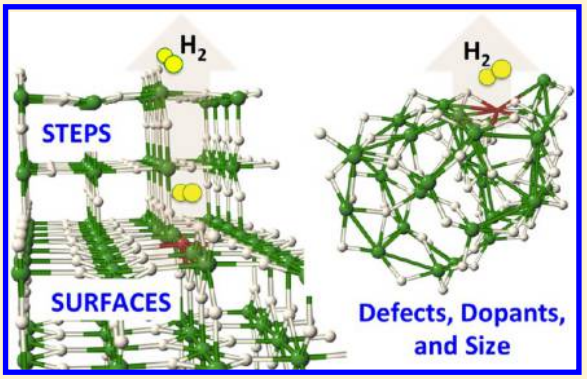

1. INTRODUCTION

At 7.6 wt % H, magnesium hydride (MgH_2) is a natural system to study in the search for an on-board solid-state H-storage material for fuel cell automobiles. However, in light of the following U.S. Department of Energy (DOE) criteria, there are two immediate issues with MgH_2 for such application. The DOE has set thermodynamic and kinetic targets for on-board hydrogen storage;[1−3] the targets correspond to a hydrogen-desorption enthalpy of ∼30 kJ/(mol H_2) and a hydrogen recharging time of under 5 min. The first issue, then, is that a temperature of 300 °C is required for MgH_2 and a solid solution of H in Mg to coexist under a gaseous H_2 pressure of 1 bar, which, with the other temperature/pressure coexistence points, corresponds to a desorption enthalpy of 76 kJ/(mol H_2),[4,5] well above the desired target. Second, with a hydrogen pressure of 10 bar, it takes ∼50 min to reach half of Mg's storage capacity at 300 °C, well outside the target recharging time.[6] Sufficient insight to tune the thermodynamic and/or kinetic behavior of the MgH_2 prototype (or related systems) compatible with H-storage material targets for automotive use remains open (see recent reviews[1,7,8]) and is the focus of the present study of equilibrium properties.

Various directions have been explored for solid-state H-storage systems in efforts to meet the on-board H-storage targets. One approach is to develop either a means to destabilize the reactants (the fully hydrated solid in the tank) or to stabilize the products;[9,10] both serve to decrease the enthalpy of H_2 release. However, with more exotic mixtures, it becomes increasingly likely that unexpected intermediate species will appear during sorption reactions; one must watch for a particularly stable intermediate that impacts or prevents recycling.[11] Also, including additives into energy-dense storage systems creates a trade-off between introducing heavy atoms and the high H-energy density.[12]

A second approach adds new species to the system to improve the kinetics of H sorption.[13,14] Here, the same trade-off applies between introducing heavy atoms and H-energy density; of course, as the former goes up, the latter goes down. In practice, depending on the type of additive and its concentration, there might be an impact on the kinetics, on the thermodynamics, or on both. Finally, one can explore if any size or geometric changes in the storage material influence its thermodynamic or kinetic properties.[12,15]

Here, to address some of the outstanding issues that remain for MgH_2 systems,[7,8,16] we directly address H-desorption enthalpies, and the energetics for breaking H−metal bonds within MgH_2 with(out) catalytic dopants. To assess size effects, e.g., relevant to ball-milled samples, we report these results for stable nanocluster geometries (found via first-principles

Received: April 26, 2012
Revised: August 17, 2012
Published: September 4, 2012

simulated annealing) and for semi-infinite bulk surfaces, both on a terrace and step edge.

2. COMPUTATIONAL DETAILS

We perform DFT total-energy calculations with the Vienna ab initio Simulation Package (VASP)[17−20] employing a plane-wave basis-set and the projector augmented wave (PAW) method.[21] We used a 400 eV kinetic energy cutoff and 8 × 8 × 12 (1 × 1 × 1, or Γ) *k*-point mesh for bulk (cluster) calculations. For $Mg_{31}H_{62}$ clusters, calculations were done using a (20 Å)^3 supercell with a minimum vacuum spacing of at least 5 Å. For all calculations, forces were converged below 0.02 eV/Å. Spin-polarized calculations were performed for systems with transition-metal dopants. Perdew−Wang generalized gradient approximation (PW91)[22] was used for the exchange-correlation functional; the same has been used to predict hydrogen-storage reactions[23] and structure[24] that match observation. A study of GGA in VASP using many metal-hydrides, including MgH_2, showed that this choice of exchange-correlation yields results that compare well to experimental formation enthalpies.[25] The bulk lattice parameters and formation energy (including zero-point (ZP) energy) for rutile MgH_2 calculated in DFT-PW91, see Table 1, are in very good agreement with experiment[26,27]

Table 1. Calculated and Observed Bulk Lattice Parameters and Formation Energy (ΔE^f) With(Out) ZP Energy for Rutile MgH_2 at 0 K; ΔE^f for Amorphous $Mg_{31}H_{62}$ Is Also Given

	ZP	system	*a* (Å)	*c*/*a*	*x*	ΔE^f (kJ/(mol H_2))
exptl			4.50	0.669	0.304	75[a]
DFT-PW91	yes	rutile bulk	4.51	0.668	0.304	52.7
	no	rutile bulk				64.3
	no	$Mg_{31}H_{62}$				70
DFT-LDA	yes	rutile bulk				85.1[b]
DFT-B97	yes	$Mg_{30}H_{60}$				72.5[c]
diffusion-QMC	yes	$Mg_{31}H_{62}$				77[b]

[a]See ref 27; this is an average desorption enthalpy at 683 K. [b]See ref 30. [c]See ref 31.

and other DFT[23,28] and quantum Monte Carlo[29,30] (which, in principle, are exact) calculations. For structural energy differences at fixed stoichiometry, e.g., from relaxation or configurational changes, the effects of ZP energy effectively cancel. Trends from PW91 versus size (cluster to bulk) without ZP energy are identical to QMC[30] but lower by ∼10 kJ/(mol H_2).

For simulated annealing, the following process was repeated iteratively. To explore the large configurational space for possible low-energy structures, we performed ab initio molecular dynamics (MD) for 200 steps with a time step of 10 fs using the Nose−Hoover thermostat at 1000 K. All atomic masses were set to 195 au to explore coordinate arrangements efficiently. Low-energy candidate configurations obtained from the potential energy versus time were fully relaxed at 0 K with proper masses. Low-energy configurations found in this way were then used as input for the next iteration, which provides reliable convergence toward lowest-energy structures.[32]

A semi-infinite surface slab was used to model the rutile MgH_2(110) surface, which can be viewed as the stacking of H−Mg−H trilayer (TL) units in the ⟨110⟩ direction; three TLs were used. All of these (110) surface calculations were done in a (4 × 2) supercell with atoms in the bottom TL fixed to their bulk-terminated positions. The vacuum spacing between the neighboring slabs is at least 12 Å. The dipole energy correction for the rutile MgH_2(110) surface was negligible at 0.06 meV.

Simulated annealing was applied to search for low-energy reconstructed configurations for the Ti-doped MgH_2(110) surface. We found a low-energy structure with a triply bonded surface H (the Ti was swapped with Fe after annealing).[32] For the step edge, a (4 × 2) supercell containing 5 TLs was used. No atoms were frozen, and the step was created by the intersection of a (110) terrace and an (001) surface. The vacuum spacing on the step edge is 13 Å. The simulated annealing procedure was critical in finding low-energy *stable* configurations for desorption calculations.

For bulk-terminated $Mg_{31}H_{62}$, the inner part of the cluster has a rutile structure, and the surface had additional H added to saturate the dangling bonds and maintain the proper stoichiometry. Simulated annealing on this structure reveals that it is unstable to the amorphous cluster.

For clusters, all single-site H-desorption energies reported were calculated as

$$\Delta E_{\mathrm{H}}^{\mathrm{des}} = E[\mathrm{Mg}_{n-1}\mathrm{X}_1\mathrm{H}_{2n-1}] + \frac{1}{2}E[\mathrm{H}_2] - E[\mathrm{Mg}_{n-1}\mathrm{X}_1\mathrm{H}_{2n}] \quad (1)$$

where X = Mg, Ti, or Fe. For the cluster, *n* is 31; for the semi-infinite (step edge) surface supercell with periodic boundary conditions, *n* is 48 (80). Depending upon the number of the local H-to-metal bonds, H-desorption energy can be significantly different. The bulk formation energy (Table 1) is calculated as

$$\Delta E^f = E^{\mathrm{hcp}}[\mathrm{Mg}] + E[\mathrm{H}_2] - E^{\mathrm{rutile}}[\mathrm{MgH}_2] \quad (2)$$

Table 1 also shows the total H-desorption energy for $Mg_{31}H_{62}$ calculated from

$$\Delta E^f = E[\mathrm{Mg}_{31}] + 31E[\mathrm{H}_2] - E[\mathrm{Mg}_{31}\mathrm{H}_{62}] \quad (3)$$

Wagemans et al.[31] reported a DFT value with ZP energies of 70 kJ/(mol H_2) for complete desorption from $Mg_{30}H_{60}$, roughly that for bulk MgH_2, see Table 1. We found a similar result for desorption (energy difference). We also confirmed a less than 12 kJ/(mol H_2) effect from ZP energies on bulk MgH_2. As such, to avoid the computational cost for each such calculation, we report our results without ZP energies.

3. RESULTS

To understand the controlling factors for hydride recycling properties, we present the effect of size and doping on the H-desorption. To accomplish this, we first present results from semi-infinite surfaces in section 3.1, i.e., both a terrace (where H is bonded to multiple metal atoms) and a step (where H is bonded to one metal atom); then we present results from stable amorphous nanoclusters in section 3.2. In section 3.3, we discuss the effects of size for (un)doped cases. In section 3.4, we discuss technical issues that result in spurious exothermic desorption energies when using finite, bulk-terminated clusters as representatives for stable nanoparticles, as done recently[33] for (un)doped MgH_2. In each section, we also address how dopants affect H-desorption energy on cluster or semi-infinite surfaces.

3.1. Desorption from Stepped Surface. To explore effects of size when moving to nanoscale MgH_2, we need semi-infinite surface results as a reference. Du et al.[34] have studied H-desorption on $MgH_2(110)$ but not for stepped surfaces, which is more relevant to experiment and nanoclusters exhibiting singly bonded H. Therefore, we calculated the H-desorption energies from the MgH_2 step edge formed between a (110) and a (001) surface, see Figure 1, with H singly bonded to Mg.

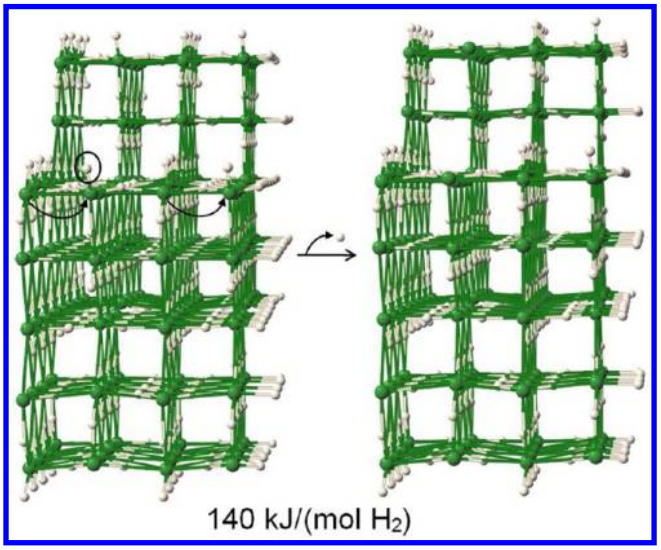

Figure 1. Before (left) and after (right) desorption of a singly bonded H from the (110)/(001) step edge for rutile MgH_2. Green (white) spheres stand for Mg (H) atoms. Pictured here is the 240 atom supercell and a reproduction of the 240 atoms by the step-translation vector to show the step, which is the intersection of the (110) surface and the (001) face orthogonal to it. The (4 × 2) supercell is 5 TLs deep with 50% coverage, via bridging H sites. The curved arrows before desorption show where two singly bonded H's were moved in order to create an initial stable structure that does not collapse during H-desorption. The H circled in black was removed to create the final state.

Before H-desorption, the curved arrows on the stepped structure indicate how two singly bonded H's are oriented to create a stable step edge. The second (110) terrace is formed by a step-translation vector of the lower terrace. The H-desorption energy for the singly bonded H on this step edge is 140 kJ/(mol H_2).

A doubly bonded H exists on the lowest-energy (110) surface of MgH_2, the terraces of a stepped surface. Figure 2 shows a doubly bonded H leaving from the undoped and Ti-doped (110) surface; they have desorption energies of 231 and 193 kJ/(mol H_2), respectively.

We find a triply bonded H on the Fe-doped reconstructed (110) surface, see Figure 3, yielding a H-desorption energy of 199 kJ/(mol H_2). We have reported elsewhere testing showing the preference for a Ti dopant to occupy a surface site on the MgH_2 surface.[35] Dopants on surface sites allow comparison to H-desorption from a doped (93 atom) nanocluster. For Fe-doping, we used a Ti-doped simulated-annealing result, replaced Ti by Fe, and then performed a full ionic relaxation. As we show below, triply bonded H is also found in Fe-doped amorphous $Mg_{31}H_{62}$. For the step edge and terraces on rutile (110) surfaces, we synopsized the (un)doped H-desorption energies in Table 2 for each bonding configuration.

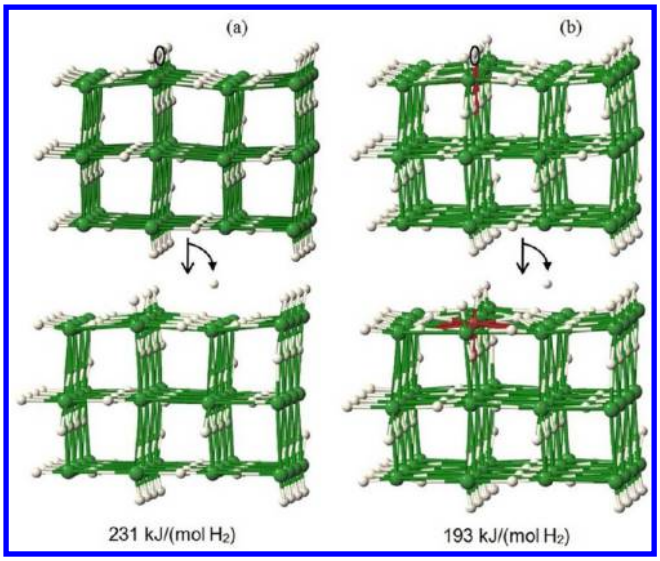

Figure 2. Desorption of a doubly bonded H from the (110) surface of MgH_2 (a) undoped and (b) Ti-doped (red atom).

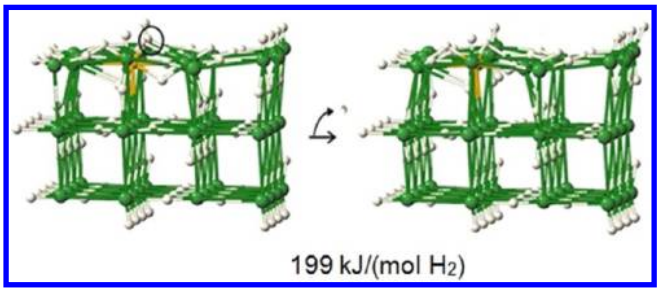

Figure 3. Desorption of a triply bonded H from a Fe-doped (orange) MgH_2 (110) surface.

Table 2. ΔE_H^{des} in kJ/(mol H_2) for Singly (s), Doubly (d), or Triply (t) Bonded H in Semi-Infinite Surfaces, Step Edges, and Clusters of (Un)Doped MgH_2[a]

		semi-infinite surfaces	amorphous cluster	bulk-terminated cluster
MgH_2	s	140*	148	143**
	d	231	252, 240, 231, 260	unstable
Ti-doped MgH_2	d	193	188	unstable
Fe-doped MgH_2	t	199, 255	208, 234	unstable

[a]Ti-doping significantly reduces the doubly bonded H-desorption energy. Bulk-terminated (mostly unstable) clusters were explored by Larsson et al.[33] (*) Step edge. (**) Only case of H-desorption not inducing significant structural change in unstable bulk-terminated cluster (see section 3.4).

3.2. Globally Stable Amorphous Clusters. The stable $Mg_{31}H_{62}$ clusters found via simulated annealing tend to have interesting amorphous structures, as found here and in another group.[36] Figure 4, a simulated annealing result, shows four different views of a $Mg_{31}H_{62}$ amorphous cluster (one with a singly bonded H that will be compared to the singly bonded H at a step). This $Mg_{31}H_{62}$ amorphous structure is 4.86 eV lower than its bulk-terminated counterpart, see section 3.4. Observe that the cluster has crowns topping off pockmarks on the surface of the particle. For recharging, assuming an amenable

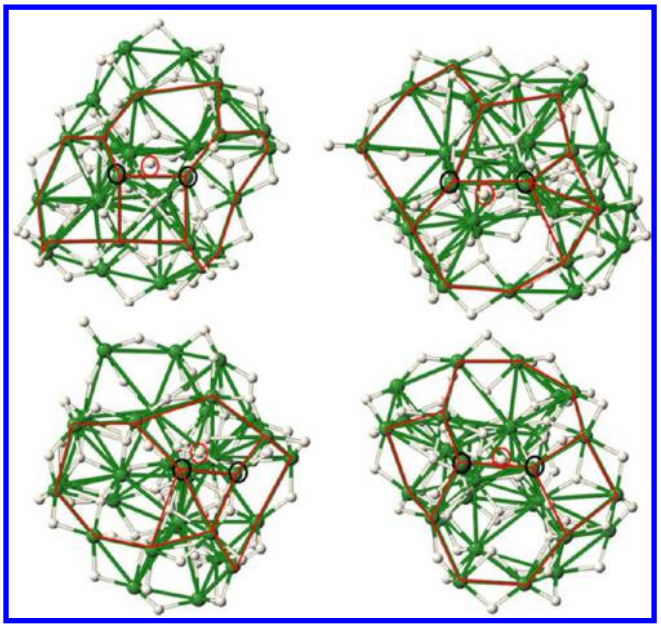

Figure 4. Four different doubly bonded H's in $Mg_{31}H_{62}$ from simulated annealing. Crowns on the surface are indicated (red lines) with the desorbing H (red circle) and the two Mg initially bonded to the desorbing H atom (black circles). Different geometric environments of the two Mg are revealed by different crowns on $Mg_{31}H_{62}$, (i.e., 4−7-membered rings of Mg). Coordinates are provided in the Supporting Information; viewing software is required to appreciate the depth of the pockmark. (The distribution of ΔE_H^{des} associated with these four H are in Figure 8 and Table 2.)

time scale and inclusion of necessary catalytic dopants, the positive curvature of the pockmarks, in this or related structures, may provide helpful steric influences on the H_2 absorption.

We highlighted several of the crowns in Figure 4. Although the pockmarks have no symmetry and the overall structure certainly appears amorphous, the local structure (focus on a single surface H) reveals a doubly bonded bridging H not unlike that found for the doubly bonded H on the $MgH_2(110)$. The local rutile bonding feature is preserved even in the amorphous structure. The calculated Mg−H pair distribution function for $Mg_{31}H_{62}$ shows Mg−H bond lengths between 1.731 and 2.78 Å, with an average value of 1.96 Å versus 1.869 Å for the bulk rutile.

In Figure 5a, one of the many doubly bonded H's is shown, and it has a desorption energy of 252 kJ/(mol H_2); due to different local environments, the doubly bonded H-desorption energies studied on this structure range from 231 to 260 kJ/(mol H_2), similar to the bulk surface value of 231 kJ/(mol H_2). However, one of the H's atop the craters of this cluster breaks the pattern; this singly bonded H, see Figure 6, has a desorption energy of 148 kJ/(mol H_2), which also compares well with the singly bonded H desorption from the bulk step edge surface of 140 kJ/(mol H_2). Hence, for undoped cases, the amorphous cluster and the bulk surface have no significant difference in ΔE_H^{des}.

For Ti- and Fe-doped MgH_2, shown in Figures 5b and 7, respectively, the lowest-energy structure we found is also amorphous with locally rutile bonding features on the crowns causing the majority of those H's to be doubly bonded. Figure 5b shows that desorption of one of the doubly bonded H's from the Ti site has a desorption energy of 188 kJ/(mol H_2), a

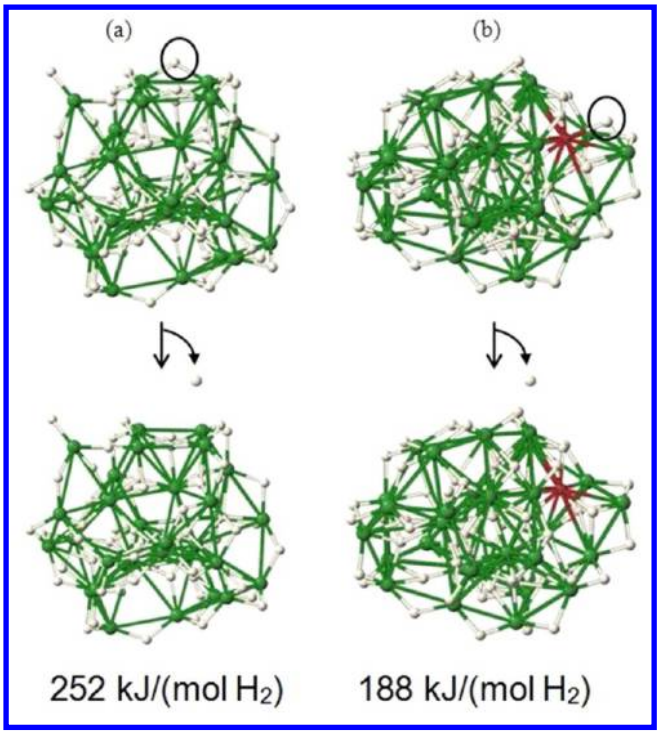

Figure 5. Desorption of a doubly bonded H from amorphous $Mg_{30}XH_{62}$, where X denotes Mg (green) or Ti (red).

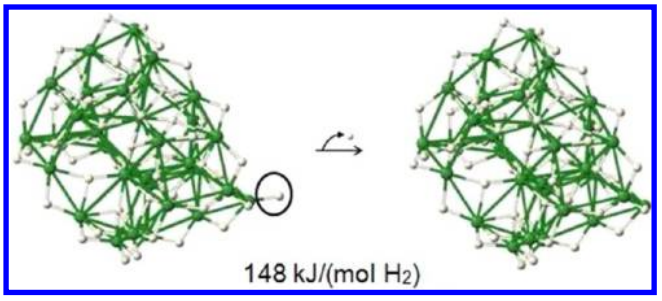

Figure 6. Desorption of a singly bonded H from the amorphous $Mg_{31}H_{62}$ cluster.

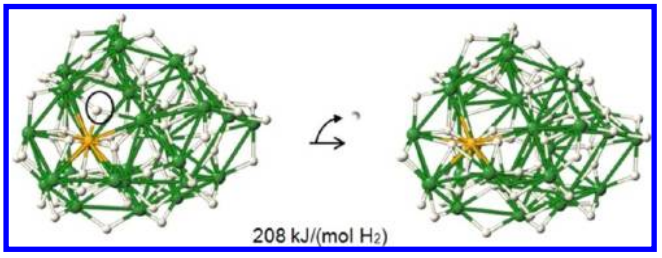

Figure 7. Desorption of a triply bonded H from the Fe-doped (orange) $Mg_{30}FeH_{62}$.

reduction of 58 kJ/(mol H_2), or 24% from the average of the undoped samples. For the Fe-doped amorphous cluster, Figure 7, the average triply bonded H desorption [from the Fe site] value is 221 kJ/(mol H_2), which is lower than the average for the undoped samples by 25 kJ/(mol H_2), a reduction of 10%. Clearly doping with Ti is effective in affecting the local bonding.

3.3. No Size Effect: Cluster versus Semi-Infinite Surface. Figure 8 summarizes all the H desorption energies from various cluster and surface structures considered in this study. The H-desorption energy is plotted versus the local

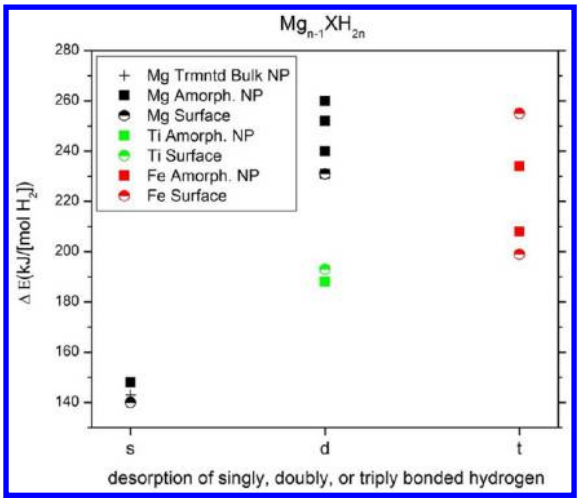

Figure 8. ΔE_H^{des} of singly, doubly, and triply bonded H from various $Mg_{31}H_{62}$ structures. "Mg Trmntd Bulk NP" is bulk-terminated after relaxation (Figure 9 from Supporting Information). "Mg/Ti/Fe Amorph. NP" refers to the stable amorphous clusters (Figures 4–7). "Mg Surface" refers to (110)/(001) step edge and (110) surface (Figures 1 and 2, respectively). "Ti (or Fe) Surface" is the relaxed (110) surface with a single Ti (Fe) substituting Mg, see Figure 2 (Figure 3).

bonding coordination for the desorbing H. Pure MgH_2 systems are shown in black, and the Ti(Fe)-doped systems are shown in green (red). The data for these three groups are also listed in Tables 2 and 3 (Table 3 appears in the Supporting Information).

The three cases showing desorption of singly bonded H from pure MgH_2 are amorphous, step-edged surface, and bulk-terminated clusters. The singly bonded H desorption from pure MgH_2 was the exceptional case where the bulk-terminated structure did not collapse (see section 3.4). All three cases show about the same desorption value of 142 kJ/(mol H_2). They differ from one another by less than 10 kJ/(mol H_2). This small change in H desorption energy shows little or no size effect. Four doubly bonded H's, chosen from the many doubly bonded H's on the amorphous $Mg_{31}H_{62}$, are shown to have desorption energies close to that of the doubly bonded H from the (110) surface. The fact that H-desorption energy for the (110) surface is at the lower bound of the four values from the amorphous cluster shows that the maximum difference of desorption energies within the same cluster is greater than or equal to the difference between the semi-infinite surface value and a cluster value. The difference between the average value from the clusters and the value from the (110) surface is smaller than 15 kJ/(mol H_2). This size effect is very small, on the order of zero-point energy.

The results from the Ti-doped amorphous cluster and Ti-doped (110) surface are very close, indicating no size effect in doped MgH_2 systems. But, comparing the undoped and Ti-doped amorphous cluster, there is a reduction in desorption energy of 58 kJ/(mol-H_2), a 24% drop. So, the catalytic dopant has a significant effect on the local metal-H bonding.

Lastly, for Fe-doped systems, the triply bonded H on the amorphous cluster and the reconstructed (110) surface both have a spread in desorption energies. The average in each case is close to the same value of 225 kJ/(mol H_2). This shows no size effect from another viewpoint: a large spread in each case indicates that the H bonding is indeed a local feature, explaining why only shrinking the overall size of the system from semi-infinite surface to a finite cluster has little effect on the local H bonding.

3.4. Bulk-Terminated Clusters: Spurious Exothermic Results. The stable bulk-terminated, 31 atom formula-unit cluster previously used to model[33] a MgH_2 nanocluster is, in fact, inherently unstable to an amorphous form, which, as shown above, is 4.86 eV lower in energy. As such, energy differences between an initial and final state from a bulk-terminated cluster do not reflect the physical desorption energetics, and spurious exothermic results can arise due to large relaxations associated with H desorption from clusters that are in a high-energy metastable state before desorption. For completeness, we reproduced these results and detailed their origin. To save space and focus on our key results, full details on this matter are provided in a section of the same name in our Supporting Information. For simplicity, the table and figure numbering within the Supporting Information continues as if the material were presented here.

4. KINETIC BARRIERS AND FUTURE CALCULATIONS

When the local bonding effects are explored in structures that are global minima, e.g., amorphous clusters, the desorption of a single H from the MgH_2 (stepped) surfaces or clusters, regardless of size, and with(out) a catalytic impurity, are consistently endothermic. How the kinetic barriers change (hopefully decrease) with dopant and size are key for altering the properties favorably for storage and release. What remains is the comparison of kinetic barriers from the amorphous clusters and from the stepped surfaces, a study that is ongoing.

Our preliminary climbing-image nudged elastic band[37,38] results in a barrier of 1.85 eV for H_2 desorption involving two bridging H's (initially on opposing sides of the crown) from amorphous $Mg_{31}H_{62}$, one of many possible pairs. For completeness, we must incorporate statistics on the geometrically unique desorption sites on the cluster.

For bulk, Du et al.[34] studied the kinetic barriers involving desorption from a bridging H site (BH) and an in-plane H site (PH) on MgH_2(110) surface and found a barrier of 1.78 eV. We have calculated[35] the desorption barriers (activation energies) on (un)doped MgH_2(110) and found a BH–PH barrier of 1.83 eV for the undoped case, and a 22% barrier reduction to 1.42 eV with Ti-doping. The decrease of the H_2 desorption barrier by 0.41 eV due to a Ti dopant (2 at. % Ti) agrees with a recent experiment[39] reporting a decrease of 0.46 eV (an 18% reduction) for ball-milled MgH_2 mixed with 1 at. % Ti. Hence, we have a very good representation of not only the thermodynamics but also the kinetics of desorption from MgH_2.

The amorphous $Mg_{31}H_{62}$ has numerous indentations with positive curvature. Identifying the class of structures and storage materials with similar curvature may be beneficial. Along with the appropriate catalytic impurities, these structures might be tuned for capturing H_2 during recharging, due to the steric influence in the indentations. Also, with a little reflection, one can see that any small cluster (up to a few hundred atoms) with a surface made up of indentations of positive curvature cannot have many atoms in its center, which reduces the diffusion distance for H.

5. CONCLUSIONS

We have provided a very good representation of the thermodynamics and kinetics of H desorption from MgH_2. We have given examples of stepped surfaces and nanoclusters, as well as full H-desorption, as compared to experiment. Using DFT simulations, we demonstrated that local bonding controls the initial H-desorption energy from any stable MgH_2 surface or stable cluster configuration. The desorption energy is ruled not by whether H is removed from semi-infinite surfaces or an amorphous nanocluster, but instead by how many metal atoms to which the desorbing H is attached; namely, for undoped singly bonded (doubly bonded) H, the desorption energy is ~140 kJ/(mol H_2) (~240 kJ/(mol H_2)). Kinetic barriers also remain similar between undoped bulk and nanoclusters, i.e., ~1.83 eV. Hence, for removing a single surface H from MgH_2, there is generally no effect from sample size on desorption energy; so the utility of ball milling is that it increases surface-to-volume ratio and distributes added dopants. For doped cases, e.g., Ti, we find a reduction on desorption energetics (−24%) and barriers (−22%) as observed, showing that transition-metal dopants do provide a catalytic effect on H desorption.

■ ASSOCIATED CONTENT

Supporting Information

Full "Bulk-Terminated Clusters: Spurious Exothermic Results" section and the coordinates of the $Mg_{31}H_{62}$ nanocluster. This material is available free of charge via the Internet at http://pubs.acs.org.

■ AUTHOR INFORMATION

Corresponding Author

*E-mail: ddj@ameslab.gov.

Notes

The authors declare no competing financial interest.

■ ACKNOWLEDGMENTS

Our work was supported by the U.S. Department of Energy, Office of Basic Energy Sciences, under contracts DEFC36-05GO15064 (Sandia Metal-Hydride Center of Excellence for J.R.) and DE-FG02-03ER15476 (Chemical Sciences, Geosciences, and Biosciences for L.L.W. and D.D.J.) and at Ames Laboratory (Complex Hydrides). Ames Laboratory is operated for the U.S. DOE by Iowa State University under contract DE-AC02-07CH11358. We also acknowledge collaborations with experimental efforts of Ian Robertson (MHCoE) and Ralph Nuzzo (catalysis) at Illinois and Vitalij Pecharsky (ball-milling and desorption) at Ames Laboratory.

■ REFERENCES

(1) Yang, J.; Sudik, A.; Wolverton, C.; Siegel, D. J. *Chem. Soc. Rev.* **2010**, *39*, 656.
(2) DOE Targets for Onboard Hydrogen Storage Systems for Light-Duty Vehicles. http://www1.eere.energy.gov/hydrogenandfuelcells/storage/pdfs/targets_onboard_hydro_storage.pdf.
(3) Reference 1 (and references therein) discuss the conversion from the DOE pressure and temperature target ranges to a target enthalpy range. Note that the current DOE pressure target range is more narrow than the one used in ref 1 to derive their target enthalpy range of 20−50 kJ/mol H_2. Also, there is a discussion about searching for enthalpy values that are consistent with high efficiency performance.
(4) Schlapbach, L.; Zuttel, A. *Nature* **2001**, *414*, 353.
(5) Akiba, E. In *Hydrogen and Fuel Cells*; Stolten, D., Ed.; Wiley-VCH: Berlin, Germany, 2010; p 395.
(6) Huot, J.; Liang, G.; Boily, S.; Van Neste, A.; Schulz, R. *J. Alloys Compd.* **1999**, *295*, 495.
(7) Sakintuna, B.; Lamari-Darkrim, F.; Hirscher, M. *Int. J. Hydrogen Energy* **2007**, *32*, 1121.
(8) Berube, V.; Radtke, G.; Dresselhaus, M.; Chen, G. *Int. J. Energy Res.* **2007**, *31*, 637.
(9) Vajo, J. J.; Mertens, F.; Ahn, C. C.; Bowman, R. C.; Fultz, B. *J. Phys. Chem. B* **2004**, *108*, 13977.
(10) Vajo, J. J.; Skeith, S. L.; Mertens, F. *J. Phys. Chem. B* **2005**, *109*, 3719.
(11) Wang, L. L.; Graham, D. D.; Robertson, I. M.; Johnson, D. D. *J. Phys. Chem. C* **2009**, *113*, 20088.
(12) Dornheim, M.; Doppiu, S.; Barkhordarian, G.; Boesenberg, U.; Klassen, T.; Gutfleisch, O.; Bormann, R. *Scr. Mater.* **2007**, *56*, 841.
(13) Bogdanovic, B. *Angew. Chem., Int. Ed.* **1985**, *24*, 262.
(14) Barkhordarian, G.; Klassen, T.; Bormann, R. *Scr. Mater.* **2003**, *49*, 213.
(15) Schulz, R.; Huot, J.; Liang, G.; Boily, S.; Lalande, G.; Denis, M. C.; Dodelet, J. P. *Mater. Sci. Eng., A* **1999**, *267*, 240.
(16) Aguey-Zinsou, K. F.; Ares-Fernandez, J. R. *Energy Environ. Sci.* **2010**, *3*, 526.
(17) Kresse, G.; Hafner, J. *Phys. Rev. B* **1993**, *47*, 558.
(18) Kresse, G.; Furthmuller, J. *Comput. Mater. Sci.* **1996**, *6*, 15.
(19) Kresse, G.; Furthmuller, J. *Phys. Rev. B* **1996**, *54*, 11169.
(20) Kresse, G.; Hafner, J. *Phys. Rev. B* **1994**, *49*, 14251.
(21) Kresse, G.; Joubert, D. *Phys. Rev. B* **1999**, *59*, 1758.
(22) Perdew, J. P.; Wang, Y. *Phys. Rev. B* **1992**, *45*, 13244.
(23) Ozolins, V.; Majzoub, E. H.; Wolverton, C. *J. Am. Chem. Soc.* **2009**, *131*, 230.
(24) Akbarzadeh, A. R.; Wolverton, C.; Ozolins, V. *Phys. Rev. B* **2009**, *79*, 184102 .
(25) Wolverton, C.; Ozolins, V.; Asta, M. *Phys. Rev. B* **2004**, *69*, 024108 .
(26) Zachariasen, W. H.; Stamper, J. F.; Holley, C. E. *Acta Crystallogr.* **1963**, *16*, 352.
(27) Bogdanovic, B.; Bohmhammel, K.; Christ, B.; Reiser, A.; Schlichte, K.; Vehlen, R.; Wolf, U. *J. Alloys Compd.* **1999**, *282*, 84.
(28) Hector, L. G.; Herbst, J. F.; Wolf, W.; Saxe, P.; Kresse, G. *Phys. Rev. B* **2007**, *76*, 014121.
(29) Pozzo, M.; Alfe, D. *Phys. Rev. B* **2008**, *77*, 104103.
(30) Wu, Z. G.; Allendorf, M. D.; Grossman, J. C. *J. Am. Chem. Soc.* **2009**, *131*, 13918.
(31) Wagemans, R. W. P.; van Lenthe, J. H.; de Jongh, P. E.; van Dillen, A. J.; de Jong, K. P. *J. Am. Chem. Soc.* **2005**, *127*, 16675.
(32) Wang, L. L.; Johnson, D. D. *Phys. Rev. B* **2007**, *75*, 235405.
(33) Larsson, P.; Araujo, C. M.; Larsson, J. A.; Jena, P.; Ahuja, R. *Proc. Natl. Acad. Sci. U.S.A.* **2008**, *105*, 8227.
(34) Du, A. J.; Smith, S. C.; Yao, X. D.; Lu, G. Q. *Surf. Sci.* **2006**, *600*, 1854.
(35) Wang, L.-L.; Johnson, D. D. *J. Phys. Chem. C* **2012**, *116*, 7874.
(36) Cheung, S.; Deng, W. Q.; van Duin, A. C. T.; Goddard, W. A. *J. Phys. Chem. A* **2005**, *109*, 851.
(37) Sheppard, D.; Terrell, R.; Henkelman, G. *J. Chem. Phys.* **2008**, *128*, 134106.
(38) Henkelman, G.; Uberuaga, B. P.; Jonsson, H. *J. Chem. Phys.* **2000**, *113*, 9901.
(39) Lu, H. B.; Poh, C. K.; Zhang, L. C.; Guo, Z. P.; Yu, X. B.; Liu, H. K. *J. Alloys Compd.* **2009**, *481*, 152.